

# Source-free Domain Adaptation Requires Penalized Diversity

Laya Rafiee Sevyeri,<sup>1,2\*</sup> Ivaxi Sheth,<sup>2,3,4</sup> Farhood Farahnak,<sup>1</sup> Alexandre See,<sup>2</sup> Samira Ebrahimi Kahou,<sup>3,4,5</sup> Thomas Fevens,<sup>1</sup> Mohammad Havaei<sup>2</sup>

<sup>1</sup> Concordia University, Montréal, Canada

<sup>2</sup> Imagia Canexia Health, Montréal, Canada

<sup>3</sup> École de Technologie Supérieure, Montréal, Canada

<sup>4</sup> Mila, Montréal, Canada

<sup>5</sup> CIFAR AI Chair

laya.rafiee@gmail.com, ivaxisheth17@gmail.com, farhood.farahnak@gmail.com, alexandre.see@imagia.com, samira.ebrahimi.kahou@gmail.com, thomas.fevens@concordia.ca, mohammad@imagia.com

## Abstract

While neural networks are capable of achieving human-like performance in many tasks such as image classification, the impressive performance of each model is limited to its own dataset. Source-free domain adaptation (SFDA) was introduced to address knowledge transfer between different domains in the absence of source data, thus, increasing data privacy. Diversity in representation space can be vital to a model’s adaptability in varied and difficult domains. In unsupervised SFDA, the diversity is limited to learning a single hypothesis on the source or learning multiple hypotheses with a shared feature extractor. Motivated by the improved predictive performance of ensembles, we propose a novel unsupervised SFDA algorithm that promotes representational diversity through the use of separate feature extractors with Distinct Backbone Architectures (DBA). Although diversity in feature space is increased, the unconstrained mutual information (MI) maximization may potentially introduce amplification of weak hypotheses. Thus we introduce the Weak Hypothesis Penalization (WHP) regularizer as a mitigation strategy. Our work proposes Penalized Diversity (PD) where the synergy of DBA and WHP is applied to unsupervised source-free domain adaptation for covariate shift. In addition, PD is augmented with a weighted MI maximization objective for label distribution shift. Empirical results on natural, synthetic, and medical domains demonstrate the effectiveness of PD under different distributional shifts.

## 1 Introduction

In recent years, the field of machine learning (ML) has witnessed immense progress in computer vision (He et al. 2016), natural language processing (Vaswani et al. 2017), and speech recognition (Bahdanau et al. 2016) due to the advances of deep neural networks (DNNs). Despite the increasing popularity of DNNs, they often perform poorly on unseen distributions (Geirhos et al. 2020), leading to overconfident and miscalibrated models. Combining the predictions of several models seems to be a feasible way to improve the generalizability of these models (Turner and Oza

\*This research was conducted during author’s internship at Imagia.

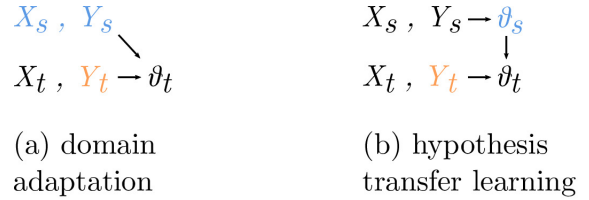


Figure 1: Transfer learning uses [accessible knowledge](#) from a source domain to inform data-driven (a) or model-driven (b) learning on a target domain. In both cases, the unsupervised setting implies that [target label data](#) is unavailable.

1999). On account of its simplicity and effectiveness, ensemble learning became popular in many machine learning applications. Due to the i.i.d. assumption that training and test sets are drawn from the same distribution, calibration (Dawid 1982) is introduced to the traditional machine learning paradigm to elucidate the model uncertainty. Additionally, predictive uncertainty is crucial under dataset shift—when confronted with a sample from a shifted distribution, an ideal model should reflect increased uncertainty in its prediction.

Commonly, a dataset distribution shift can occur due to diverse sources (Quiñero-Candela et al. 2008): (i) domain shift, also known as covariate shift, is caused by hardware differences in data acquisition devices; (ii) feature distribution disparity is caused by population-level differences (e.g., gender, ethnicity) across domains; (iii) label distribution shift, where the proportional prevalence of labels in the source domain differs from that of the target domain. Due to the variety of distribution shifts, models have failed in real-world applications with shifted domains, thus posing an important threat to safety-critical applications.

Hypothesis transfer learning (HTL), also referred to as source-free domain adaptation (SFDA), addresses distribution shift under the non-transductive setting by using knowledge encoded in a model pretrained on the source domain to inform learning on the target domain (Fig. 1b). Unlike traditional domain adaptation (DA) approaches (Fig. 1a), SFDA models do not have simultaneous access to the data from

both source and target domains. This assumption mitigates the privacy and storage concerns arising in conventional DA methods (see Fig. 1 for the difference).

Extending ensemble learning to DA frameworks and, in particular, SFDA methods can uncover multiple modes within the source domain, improving the transferability of these models (Lao, Jiang, and Havaei 2021). However, the performance gain of an ensemble model is largely related to the diversity of its members. Particularly, averaging over identical networks or ensemble members with limited diversity is not better than a single model (Rame and Cord 2021).

In this work, we encourage diversity among ensemble members in an unsupervised source-free domain adaptation setting where no labeled target data is available. While recent work in unsupervised SFDA has shown promising results, they either rely on a unique feature extractor (Liang, Hu, and Feng 2020), or one shared between an ensemble of source hypotheses (Lao, Jiang, and Havaei 2021), which leads to limited diversity in the function space of the source domain (see Sec. 3.5 for analysis).

Diversity in ensemble leads to the best-calibrated uncertainty estimators (Lakshminarayanan, Pritzel, and Blundell 2017), and therefore the performance benefits of feature diversity within ensembles in out-of-distribution (OOD) settings (Pagliardini et al. 2022). Other recent works in DNN analysis also show that different architectures tend to explore different representations (Kornblith et al. 2019; Nguyen, Raghu, and Kornblith 2021; Antorán, Allingham, and Hernández-Lobato 2020; Zaidi et al. 2021). Inspired by them, our work proposes to increase diversity by not only using separate feature extractors but also by introducing Distinct Backbone Architectures (DBA) across hypotheses.

While a regularization approach to unconstrained mutual information (MI) maximization during adaptation is promising in low diversity settings (Lao, Jiang, and Havaei 2021), enforcing similarity between highly diverse hypotheses is insufficient to counteract the catastrophic impact of weak hypotheses when they inevitably arise as outliers. Therefore, we highlight the necessity of a trade-off between diversity and the amount of freedom each ensemble member can have. Hence, we introduce Penalized Diversity (PD), a new unsupervised SFDA approach that maximizes diversity exploitation via DBA while mitigating the negative impact of Weak Hypotheses through the Penalization (WHP) of their contribution by regularization.

In many real-world applications, the uniform distribution assumption between source and target does not hold. This assumption can negatively impact the performance of many current SFDA models under label distribution shift (Liang, Hu, and Feng 2020; Lao, Jiang, and Havaei 2021) (Sec. 3.4, label shift experiments). We further extend PD to address the label distribution shift by introducing a weighted MI maximization based on estimation over target distribution. Extensive experiments on multiple domain adaptation benchmarks (Office-31, Office-Home, and VisDA-C), medical, and digit datasets under covariate and label distribution shifts exhibit the effectiveness of PD.

## 2 Approach

### 2.1 Preliminaries

Assuming  $\mathcal{X}$  indicates the input space and  $\mathcal{Y}$  represents the output space, in an unsupervised source-free domain adaptation (uSFDA) setting, we denote the source domain as  $\mathcal{D}_s = \{(x_i^S, y_i^S)\}_{i=1}^{N_s}$ , where  $x_i^S \in \mathcal{X}^S$  and  $y_i^S \in \mathcal{Y}^S$ . The unlabeled target domain is denoted as  $\mathcal{D}_t = \{(x_i^T)\}_{i=1}^{N_t}$ , where  $x_i^T \in \mathcal{X}^T$  and  $\mathcal{X}^S \neq \mathcal{X}^T$ . For now, we assume that the difference in the joint distribution  $P(\mathcal{X}, \mathcal{Y})$  of source and target stems from the covariate shift only. Therefore, this induces a domain shift between the source and target domains, ( $P_S(X) \neq P_T(X)$ ), whereas the learning task remains the same, with  $\mathcal{Y}^S = \mathcal{Y}^T$  and  $P_S(Y | X) = P_T(Y | X)$ . Given a hypothesis space  $\mathcal{H}$ , uSFDA learns a source hypothesis  $h_s : \mathcal{X}^S \rightarrow \mathcal{Y}^S \in \mathcal{H}^S$  and a target hypothesis  $h_t : \mathcal{X}^T \rightarrow \mathcal{Y}^T \in \mathcal{H}^T$ , to predict the unobserved target labels  $Y_t^*$ . From the Bayesian perspective, the predictive posterior distribution can be written as:

$$\begin{aligned} p(Y_t^* | \mathcal{D}_s, \mathcal{D}_t) \\ = \int_{h_t} p(Y_t^* | \mathcal{D}_t, h_t) \int_{h_s} p(h_t | \mathcal{D}_t, h_s) p(h_s | \mathcal{D}_s) dh_s dh_t \end{aligned} \quad (1)$$

Eq. 1 describes two learning phases; first, the posterior over the source hypothesis  $p(h_s | \mathcal{D}_s)$  is learned using the source dataset  $\mathcal{D}_s$ , and second, the posterior over the target hypothesis  $p(h_t | \mathcal{D}_t, h_s)$  is learned by marginalizing over samples of the source hypothesis adapted to the target domain, which only contains unlabeled examples.

Liang, Hu, and Feng (2020) use a single model to estimate the distribution over the source hypothesis, and by extension the distribution over the target hypothesis. Lao, Jiang, and Havaei (2021) improved this approximation by incorporating multiple hypotheses that *share* the same feature extraction backbone. While the latter is considered an ensemble, by definition, it is constrained by learning shared extracted features. In this paper, we promote diversity by introducing the use of Distinct Backbone Architectures (DBA) across hypotheses. We argue and show empirically (Sec. 3.4) that this helps us achieve a better approximation of  $p(h_t | \mathcal{D}_t, h_s)$  with higher diversity in the representation space.

However, unconstrained MI maximization during adaptation is prone to the induction of weak hypotheses due to error accumulation. The hypothesis disparity (HD) introduced by (Lao, Jiang, and Havaei 2021) acts as a regularizer by enforcing similarity across hypotheses over the distribution of predicted labels. While this regularization showed promise in low diversity settings, enforcing similarity between highly diverse hypotheses is insufficient, and weak hypotheses inevitably arise (see Sec. 3.5 for experiments). Unfortunately, the very nature of how similarity is computed in HD makes it highly vulnerable to weak hypotheses. We propose an approach that mitigates the negative impact of Weak Hypotheses through the Penalization (WHP) of their contribution to the computation of HD when they arise as outliers (Sec. 3.4).

In the following sections, we describe three main components of our proposed model, Penalized Diversity (PD).

## 2.2 Learning Diverse Source Hypotheses Using Distinct Backbone Architectures

To maximize the diversity of predictive features learned in the source domain, we propose removing any weight sharing between the backbones of separate hypotheses by introducing the use of distinct architectures. For example, on the LIDC dataset, our approach (DBA) is implemented through the use of a mixture of ResNet10 and ResNet18 backbones.

We define the set of source hypotheses as  $\{h_i^S : h_i^S = f_i^S \circ g_i^S\}_{i=1}^M$ , where  $\{f_i^S\}_{i=1}^M$  and  $\{g_i^S \in \Psi^S\}_{i=1}^M$  represent the set of classifiers and the set of feature extractors, respectively, and  $M$  represents the number of hypotheses. We train each hypothesis using the cross entropy loss function ( $CE$ ):

$$L_S = \arg \min_{\mathcal{H}^S} \mathbb{E}_{(x,y) \in \mathcal{X}^S \times \mathcal{Y}^S} [CE(h(x), y)], \forall h \in \{h_i^S\}_{i=1}^M \quad (2)$$

where  $h(x) = p(y | x; h)$  denotes the probability distribution of input  $x$  predicted by hypothesis  $h$ .

## 2.3 Diversity Exploitation Through Weak Hypothesis Penalization

Assuming  $\mathcal{D}_t = \{(x_i^T)\}_{i=1}^{N_t}$  is a set of unlabeled target samples, our goal is to effectively adapt the set of hypotheses trained on the source domain  $\{h_i^S\}_{i=1}^M$  into a set of target hypotheses  $\{h_i^T\}_{i=1}^M$ . Due to the absence of both source data and labeled target data during the adaptation phase, we maximize the mutual information (MI) between the target data distribution ( $X^T$ ) and the predictions by the target hypotheses ( $\hat{Y}^T$ ) (Liang, Hu, and Feng 2020) using Eq. 3.

$$\max_{\Psi^T} \mathbb{E}_{x \in \mathcal{X}^T} [I(X^T; h(X^T))], \forall h \in \{h_i^T\}_{i=1}^M \quad (3)$$

where  $I(X^T; \hat{Y}^T) = H(\hat{Y}^T) - H(\hat{Y}^T | X^T)$  is defined as MI with  $H$  indicating entropy,  $\hat{Y}^T$  is the predicted output of  $h(X^T)$ , and  $\Psi^T$  is the space of target feature extractors. Assuming that only covariate shift is present, both the source and the target domains share the same label space, so we keep the parameters for the classifiers  $f_i^T$  fixed while updating the feature extractors  $g_i^T \in \Psi^T$ .

Unconstrained unsupervised training of target hypothesis ensembles solely using MI maximization results in undesirable target label prediction disagreements. We use the hypothesis disparity (HD) regularization to marginalize out these disagreements (Lao, Jiang, and Havaei 2021). HD measures the dissimilarity between the predicted label probability distributions among pairs of hypotheses over the input space  $\mathcal{X}$ :

$$\text{HD}_{h_i, h_j \in \{h^T\}, i \neq j} (h_i, h_j) = \int_{\mathcal{X}} d(h_i(x), h_j(x)) p(x) dx \quad (4)$$

where  $d(\cdot)$  defines the dissimilarity metric. Throughout this study, we use cross entropy to measure dissimilarity.

In its original formulation, computing HD relies on randomly selecting a single hypothesis that serves as an anchor (reference) for the pairwise disparity measures with the rest of the  $M-1$  hypotheses. This selected anchor remains fixed throughout the training process. We note that this method of

choosing the anchor may potentially have a catastrophic impact; a weak performance hypothesis chosen as the anchor could act as an attractor and collapse the model (See 3.5 and Table 7).

In order to address this issue, we redefine HD (Eq. 4) by proposing Weak Hypothesis mitigation through Penalization (WHP), which constructs the anchor hypothesis ( $h_{\text{whp}}$ ) as an ensemble where the contribution of each hypothesis is weighted according to its cosine similarity to other hypotheses (Eq. 5 to Eq. 8):

$$h_{\text{whp}}(X^T) = \sum_{i=1}^M \hat{w}_i h_i(X^T), \quad (5)$$

where  $h_i \in \{h^T\}$ , and  $\hat{w}_i$  represents the normalized weight for each hypothesis and is computed as:

$$\hat{w}_i = \frac{\exp(w_i)}{\sum_{j=1}^M \exp(w_j)} \quad (6)$$

$$w_i = \mathbb{E}_{h_j \in \{h^T\}, j \neq i} \left[ \frac{h_i(X^T) \cdot h_j(X^T)}{|h_i(X^T)| \cdot |h_j(X^T)|} \right], \forall i. \quad (7)$$

$$\text{HD}_{h_i \in \{h^T\}} (h_i, h_{\text{whp}}) = \int_{\mathcal{X}} d(h_i(x), h_{\text{whp}}(x)) p(x) dx \quad (8)$$

In effect, the contribution to the ensemble anchor  $h_{\text{whp}}$  of a more distant hypothesis  $h_i$ , based on its marginal cosine similarity to other hypotheses, is penalized through the reduction of  $w_i$ . Hence, we improve performance by diminishing the probability of selecting a weak anchor. In Section 3.5, we compare WHP to alternative strategies for anchor hypothesis selection and show its superior performance.

## 2.4 Target Distribution Estimation Via Pseudo-Labels

We take one step further and refine our assumption on possible shifts in the joint distribution of source and target. Instead of assuming that the changes only stemmed from the difference in their marginal ( $P(X)$ ), we also allow shifts in their prior, i.e.  $P_S(Y) \neq P_T(Y)$ , namely label distribution shift. For PD to be able to perform under label distribution shift, we suggested weighted mutual information (MI) based on the proportion of target classes. Since the exact proportion of target classes is not accessible in an unsupervised setting, an estimation using pseudo-labeling (Liang, Hu, and Feng 2020) can be used. The label entropy for MI maximization is reweighted according to the estimated class proportions and reformulates the MI maximization as:

$$I_W(X^T; \hat{Y}^T) = W * H(\hat{Y}^T) - H(\hat{Y}^T | X^T) \quad (9)$$

where  $W = [w_1, \dots, w_C]$  is an estimated class proportion from pseudo-labels, and  $w_i = \frac{n_{c_i}}{\sum_{j=1}^C n_{c_j}}$ , where  $n_{c_i}$  represents the number of samples in class  $c_i$  and  $C$  is the total number of classes.

In summary, our full objective for target training is a combination of weighted mutual information and hypothesis disparity regularization.

$$L_T = \alpha \mathbb{E}_{h \in \mathcal{H}^T} [-I_W(X^T; h(X^T))] + \beta \mathbb{E}_{h \in \{h^T\}} [\text{HD}(h, h_{\text{whp}})] \quad (10)$$

where  $\alpha$  and  $\beta$  are hyperparameters indicating the contribution of each of MI and HD in the target training.

## 3 Experiments and Results

### 3.1 Datasets

To validate our model under covariate shift, we consider natural and medical image datasets. For the natural images, we consider domain adaptation benchmark datasets, namely **Office-31** (Saenko et al. 2010), **Office-Home** (Venkateswara et al. 2017), and **VisDA-C** (Peng et al. 2018). For the medical application, we evaluate our model on the **LIDC** (Armatto III et al. 2011) dataset. Office-31 dataset includes three domains that share a set of 31 classes; Amazon (A), DSLR (D), and Webcam (W). Office-Home has four domains, each having 65 classes; Artistic images (AR), Clip art (CL), Product images (PR), and Real-World images (RW). VisDA-C has 12 classes with synthetic images in the source domain and real images in the target domain. For our medical imaging experiment, we divided the LIDC dataset into four domains based on the manufacturer of the data-capturing device: GE.medical (G), Philips (P), SIEMENS (S), and TOSHIBA (T). Each of these domains has two classes, healthy and unhealthy. We validate the existence of covariate shift across LIDC domains, from both statistical and experimental perspectives. A detailed statistical analysis is provided in the Appendix A. For the experiments on label shift, we consider synthetic digit datasets—**MNIST** (M) (LeCun et al. 1998), **MNIST-M** (N) (Ganin et al. 2016), and **USPS** (U) (Hull 1994).

### 3.2 Baselines

Unsupervised transfer learning approaches can be categorized as either unsupervised domain adaptation (UDA) or SFDA, depending on whether or not they require access to the source data during the adaptation phase. We consider baselines from both sets. For UDA, we compare PD to DANN (Ganin and Lempitsky 2015), DAN (Long et al. 2015), CDAN (Long et al. 2018), SAFN+ENT (Xu et al. 2019), rRevGrad+CAT (Deng, Luo, and Zhu 2019), MDD (Zhang et al. 2019), and MCC (Jin et al. 2020). For SFDA, we use AdaBN (Li et al. 2016), Tent (Wang et al. 2021), SHOT (Liang, Hu, and Feng 2020), HDMI (Lao, Jiang, and Havaei 2021), and NRC (Yang et al. 2021). We also consider the performance of source hypotheses at directly predicting target labels as a Source-only model, and MI-ensemble as a model with three hypotheses with only MI maximization and no regularizer.

For label distribution shift experiments, aside from comparing with two SFDA models namely SHOT and HDMI, we compare PD with MARS (Rakotomamonjy et al. 2022) and OSTAR (Kirchmeyer et al. 2022), the two recent state-of-the-art models for label distribution shift. MARS (Rakotomamonjy et al. 2022) proposed based on two estimating

proportion strategies, where hierarchical clustering defines MARS<sub>c</sub> and Gaussian mixtures indicates MARS<sub>g</sub>. In nearly all our experiments, MARS<sub>c</sub> outperforms MARS<sub>g</sub>, therefore we only report the performance of MARS<sub>c</sub> while referring to it as MARS.

### 3.3 Experimental Setup

In the experiments presented in this paper, we consider both covariate shift and label distribution shift between source and target domains. We simply instill diversity in DBA using different depths of a given architecture (Antorán, Allingham, and Hernández-Lobato 2020; Zaidi et al. 2021). The code base of PD is built upon SHOT. Further details on the hyperparameters are provided in the Appendix A.

### 3.4 Results

In this section, we present the performance of our model in comparison with the baselines in each benchmark dataset under different distributional shifts.

**Natural Images** The performance of our model alongside the baselines on Office-31, Office-Home, and VisDA-C under covariate shift are presented in Table 1, 2, and 4 respectively, where it can be observed that our Penalized Diversity (PD) approach outperforms all UDA and SFDA baselines.

**Medical Dataset** The experimental results on the LIDC dataset, given four different domains, are depicted in Table 3. The results indicate the effectiveness of PD in comparison with other baselines. Using DBA with WHP increases the performance from 62.3% to 63.5%.

**Digit Dataset** The effect of using weighted label entropy in our modified MI maximization objective in the experiments on digit datasets is presented in Table 5. Following (Azizzadenesheli et al. 2019), we used two strategies, namely *Tweak-One shift* and *Minority-Class shift* with a probability value of  $p$  to create a label distribution shift in each of the datasets. In *Tweak-One shift* ( $L_t$ ), one of the classes is randomly selected whereas, in *Minority-Class shift* ( $L_m$ ), a subset of classes (in our experiments, 5 out of 10 classes) is chosen randomly. Then the proportion of the chosen class(es) in the target domain changes by value  $p$ , i.e. keeping only  $p\%$  of the samples in the chosen class (see Fig. 4 (b) and (c) for the distribution of labels in each dataset). As demonstrated in Table 5, using an estimation of target label distribution as weights in MI objective mitigates the impact of label shift. The improvement is more notable in  $L_m$  experiment (more than 8% improvement over OSTAR). In these experiments, covariate shift is also present.

### 3.5 Analysis

**DBA increases the diversity of source hypotheses** In order to investigate the relative impact on the diversity of introducing separate source hypothesis backbones with the same architecture and using distinct backbone architectures, we follow (Fort, Hu, and Lakshminarayanan 2019) and measure the source hypotheses’ disagreement in function space.

Table 1: Target accuracy (%) on Office-31 under covariate shift (source  $\rightarrow$  target). In this and all the following tables,  $\dagger$  represents results reported from our implementations.

Method	Source-free	A $\rightarrow$ D	A $\rightarrow$ W	D $\rightarrow$ A	D $\rightarrow$ W	W $\rightarrow$ A	W $\rightarrow$ D	Avg.
Source-only $\dagger$	×	78.6	80.5	63.6	97.1	62.8	99.6	80.4
DAN (Long et al. 2015)	×	78.6	80.5	63.6	97.1	62.8	99.6	80.4
DANN (Ganin and Lempitsky 2015)	×	79.7	82.0	68.2	96.9	67.4	99.1	82.2
SAFN+ENT (Xu et al. 2019)	×	90.7	90.1	73.0	98.6	70.2	99.8	87.1
rRevGrad+CAT (Deng, Luo, and Zhu 2019)	×	90.8	94.4	72.2	98.0	70.2	<b>100.</b>	87.6
MDD (Zhang et al. 2019)	×	93.5	<b>94.5</b>	74.6	98.4	72.2	<b>100.</b>	88.9
MCC (Jin et al. 2020)	×	95.5	98.6	100	94.4	72.9	74.9	89.4
MI-ensemble $\dagger$	✓	91.0	93.0	72.3	96.5	73.7	97.4	87.3
AdaBN (Li et al. 2016)	✓	81.0	82.4	67.2	97.7	68.2	99.8	82.7
Tent (Wang et al. 2021)	✓	82.1	85.1	68.8	97.5	63.0	99.8	82.7
SHOT (Liang, Hu, and Feng 2020)	✓	93.1	90.9	74.5	98.8	74.8	99.9	88.7
HDMI (Lao, Jiang, and Havaei 2021)	✓	94.4	94.0	73.7	98.9	75.9	99.8	89.5
NRC (Yang et al. 2021)	✓	<b>96.0</b>	90.8	<b>75.3</b>	<b>99.0</b>	75.0	<b>100.</b>	89.4
PD	✓	95.6	94.3	<b>75.3</b>	98.7	<b>76.4</b>	99.8	<b>90.0</b>

Table 2: Target accuracy (%) on Office-Home under covariate shift (source  $\rightarrow$  target).

Method	Source-free	Ar $\rightarrow$ Cl	Ar $\rightarrow$ Pr	Ar $\rightarrow$ Rw	Cl $\rightarrow$ Ar	Cl $\rightarrow$ Pr	Cl $\rightarrow$ Rw	Pr $\rightarrow$ Ar	Pr $\rightarrow$ Cl	Pr $\rightarrow$ Rw	Rw $\rightarrow$ Ar	Rw $\rightarrow$ Cl	Rw $\rightarrow$ Pr	Avg.
Source-only $\dagger$	×	45.6	69.2	76.5	55.3	64.4	67.4	55.1	41.6	74.4	66.0	46.3	79.4	61.8
DAN (Long et al. 2015)	×	43.6	57.0	67.9	45.8	56.5	60.4	44.0	43.6	67.7	63.1	51.5	74.3	56.3
DANN (Ganin and Lempitsky 2015)	×	45.6	59.3	70.1	47.0	58.5	60.9	46.1	43.7	68.5	63.2	51.8	76.8	57.6
SAFN (Xu et al. 2019)	×	52.0	71.7	76.3	64.2	69.9	71.9	63.7	51.4	77.1	70.9	57.1	81.5	67.3
MDD (Zhang et al. 2019)	×	54.9	73.7	77.8	60.0	71.4	71.8	61.2	53.6	78.1	72.5	<b>60.2</b>	82.3	68.1
MI-ensemble $\dagger$	✓	55.2	71.9	80.2	62.6	76.8	77.8	63.2	53.8	81.1	67.9	58.3	81.4	69.2
AdaBN (Li et al. 2016)	✓	50.9	63.1	72.3	53.2	62.0	63.4	52.2	49.8	71.5	66.1	56.1	77.1	61.5
Tent (Wang et al. 2021)	✓	47.9	66.0	73.3	58.8	65.9	68.1	60.2	47.3	75.4	70.8	54.0	78.7	63.9
SHOT (Liang, Hu, and Feng 2020)	✓	56.9	78.1	81.0	67.9	78.4	78.1	67.0	54.6	81.8	73.4	58.1	<b>84.5</b>	71.6
HDMI (Lao, Jiang, and Havaei 2021)	✓	57.8	76.7	81.9	67.1	78.8	<b>78.8</b>	66.6	55.5	82.4	73.6	59.7	84.0	71.9
NRC (Yang et al. 2021)	✓	57.7	<b>80.3</b>	<b>82.0</b>	68.1	<b>79.8</b>	78.6	65.3	56.4	83.0	71.0	58.6	85.6	72.2
PD	✓	<b>58.9</b>	78.0	80.9	<b>69.3</b>	76.7	76.9	<b>69.6</b>	<b>56.5</b>	<b>83.4</b>	<b>75.1</b>	59.9	<b>84.5</b>	<b>72.5</b>

Table 3: Target accuracy (%) on LIDC under covariate shift (source  $\rightarrow$  target). The results are averaged over five different runs.

Method	Source-free	G $\rightarrow$ P	G $\rightarrow$ S	G $\rightarrow$ T	P $\rightarrow$ G	P $\rightarrow$ S	P $\rightarrow$ T	S $\rightarrow$ G	S $\rightarrow$ P	S $\rightarrow$ T	T $\rightarrow$ G	T $\rightarrow$ P	T $\rightarrow$ S	Avg.
Source-only $\dagger$	×	65.6	65.9	45.9	61.9	60.5	49.3	65.2	66.9	57.1	50.0	50.0	50.0	57.2
DAN (Long et al. 2015) $\dagger$	×	59.3	65.8	33.9	61.1	59.7	30.7	56.9	58.6	40.2	48.7	45.9	47.6	50.7
MDD (Zhang et al. 2019) $\dagger$	×	64.1	63.6	57.7	54.7	59.8	47.7	<b>67.2</b>	63.4	59.1	50.0	50.3	50.0	57.3
MI-ensemble $\dagger$	✓	67.1	63.4	<b>66.6</b>	62.9	63.2	52.1	65.1	64.9	55.2	60.8	58.6	58.2	61.5
SHOT (Liang, Hu, and Feng 2020) $\dagger$	✓	67.0	<b>67.1</b>	61.6	59.9	56.9	53.2	66.8	<b>69.0</b>	66.1	60.4	61.0	54.9	61.9
HDMI (Lao, Jiang, and Havaei 2021) $\dagger$	✓	67.1	66.6	64.6	65.4	64.2	54.6	66.2	65.1	54.6	60.7	<b>60.0</b>	58.7	62.3
PD	✓	<b>68.9</b>	65.9	60.9	<b>65.6</b>	<b>65.6</b>	<b>54.8</b>	65.8	66.9	<b>66.6</b>	<b>61.2</b>	59.6	<b>59.6</b>	<b>63.5</b>

Table 4: Target accuracy (%) on VisDA-C under covariate shift.

Method	Source-free	Avg. per-class accuracy
Source-only $\dagger$	×	44.6
DAN (Long et al. 2015)	×	61.1
CDAN (Long et al. 2018)	×	70.0
MDD (Zhang et al. 2019)	×	74.6
MCC (Jin et al. 2020)	×	78.8
Tent (Wang et al. 2021)	✓	65.7
SHOT (Liang, Hu, and Feng 2020)	✓	79.6
HDMI (Lao, Jiang, and Havaei 2021)	✓	82.4
PD	✓	<b>83.8</b>

More specifically, given a set of target samples  $X$ , we compute  $\frac{1}{N} \sum_{i=1}^M \sum_{j=1}^M [f(X; \theta_i) \neq f(X; \theta_j)]$ , where  $N$  is the total number of target samples,  $M$  defines the number of hypotheses, and  $f(\cdot)$  indicates the predicted class. Note that in this experiment, we analyze the diversity of the source hypotheses and no adaptation to the target dataset is made. We consider three ways of constructing the ensemble: 1) shared feature extractors, referred to as Shared Backbone (ShB), 2) hypotheses that are given separate feature extractors with the same backbone architecture, referred to as Separate Backbone (SeB), and 3) DBA (used in PD), which has separate feature extractors with distinct backbones. Figure 2 shows that simply introducing separate feature extractors for each hypothesis (SeB) leads to a marked increase in diversity compared to sharing a feature extractor (ShB), as in HDMI. However, the largest diversity increase comes from the in-

Table 5: Target accuracy (%) on digit datasets with no label shift ( $N_t$ ), tweak-one ( $L_t$ ), and minority-class ( $L_m$ ) label distribution shift with  $p = 0.1$  (source  $\rightarrow$  target).

Method	Strategy	Source-free	M $\rightarrow$ U	M $\rightarrow$ N	U $\rightarrow$ M	U $\rightarrow$ N	N $\rightarrow$ M	N $\rightarrow$ U	Avg.
OSTAR (Kirchmeyer et al. 2022) <sup>†</sup>	$N_t$	×	96.5	33.2	<b>98.4</b>	34.0	<b>98.4</b>	90.3	75.1
MARS (Rakotomamonjy et al. 2022) <sup>†</sup>		×	92.3	40.1	96.8	<b>38.6</b>	95.4	88.2	75.2
SHOT (Liang, Hu, and Feng 2020) <sup>†</sup>		✓	88.9	45.9	93.2	29.7	95.4	88.5	73.6
HDMI (Lao, Jiang, and Havaei 2021) <sup>†</sup>		✓	95.2	49.6	95.0	26.5	96.2	93.1	75.9
PD		✓	<b>96.9</b>	<b>50.1</b>	95.6	26.4	96.6	<b>97.6</b>	<b>77.2</b>
OSTAR (Kirchmeyer et al. 2022) <sup>†</sup>	$L_t$	×	94.6	37.9	<b>98.3</b>	27.1	<b>97.4</b>	85.6	73.5
MARS (Rakotomamonjy et al. 2022) <sup>†</sup>		×	97.4	44.4	96.2	<b>44.6</b>	90.9	89.0	<b>77.0</b>
SHOT (Liang, Hu, and Feng 2020) <sup>†</sup>		✓	84.5	46.2	89.3	30.6	89.5	83.6	70.6
HDMI (Lao, Jiang, and Havaei 2021) <sup>†</sup>		✓	89.9	48.7	89.6	27.3	90.5	87.2	72.2
PD		✓	<b>97.6</b>	<b>49.1</b>	92.9	29.1	96.4	<b>97.0</b>	<b>77.0</b>
OSTAR (Kirchmeyer et al. 2022) <sup>†</sup>	$L_m$	×	58.6	37.1	<b>96.5</b>	23.1	84.1	67.4	61.1
MARS (Rakotomamonjy et al. 2022) <sup>†</sup>		×	59.9	23.3	92.6	<b>35.3</b>	80.0	69.3	60.1
SHOT (Liang, Hu, and Feng 2020) <sup>†</sup>		✓	57.1	43.9	58.2	28.7	60.9	56.7	50.9
HDMI (Lao, Jiang, and Havaei 2021) <sup>†</sup>		✓	62.4	46.0	60.1	25.2	62.6	58.9	52.5
PD		✓	<b>87.5</b>	<b>47.7</b>	84.3	31.8	<b>85.0</b>	<b>78.6</b>	<b>69.2</b>

Table 6: Ablation study on anchor selection under covariate shift: target accuracy (%) on LIDC dataset with DBA under different anchor selection strategies (source  $\rightarrow$  target). 3H represents models with 3 hypotheses. The results are averaged over five different runs.

Method	G $\rightarrow$ P	G $\rightarrow$ S	G $\rightarrow$ T	P $\rightarrow$ G	P $\rightarrow$ S	P $\rightarrow$ T	S $\rightarrow$ G	S $\rightarrow$ P	S $\rightarrow$ T	T $\rightarrow$ G	T $\rightarrow$ P	T $\rightarrow$ S	Avg.
3H-Fixed	68.1	<b>66.5</b>	60.7	64.5	64.2	55.5	65.4	<b>67.8</b>	58.6	59.7	58.5	59.1	62.4
3H-Random	<b>69.3</b>	65.7	<b>64.5</b>	64.9	64.3	<b>55.6</b>	<b>66.4</b>	66.8	57.3	60.4	58.5	<b>59.9</b>	62.8
3H-Ensemble	69.2	66.2	59.3	65.3	64.7	54.2	65.9	67.1	56.9	61.0	59.9	<b>59.9</b>	62.6
3H-WHP	68.9	65.9	60.9	<b>65.6</b>	<b>65.6</b>	54.8	65.8	66.9	<b>66.6</b>	<b>61.2</b>	<b>59.6</b>	59.6	<b>63.5</b>

Table 7: Ablation study on anchor selection under covariate shift: target accuracy (%) on Office-31 dataset with DBA (3 hypotheses) under different anchor selection strategies (source  $\rightarrow$  target).

Method	A $\rightarrow$ D	A $\rightarrow$ W	D $\rightarrow$ A	D $\rightarrow$ W	W $\rightarrow$ A	W $\rightarrow$ D	Avg.
Fixed	94.2	93.8	71.1	98.5	71.0	<b>99.8</b>	88.1
Random	94.0	94.1	70.3	98.5	70.4	<b>99.8</b>	87.9
Ensemble	95.4	94.2	71.5	98.5	71.1	<b>99.8</b>	88.4
WHP	<b>95.6</b>	<b>94.3</b>	<b>75.3</b>	<b>98.7</b>	<b>76.4</b>	<b>99.8</b>	<b>90.0</b>

roduction of DBA.

To further examine the diversity of different ways of constructing the ensemble in the target adaption phase, we show one learning curve example for each model using fixed anchor selection (HDMI objective) in Figure 3. As expected, ShB leads to the lowest diversity. Introducing separate backbones (SeB and DBA) induces diversity that leads to an increase in performance. Furthermore, adding a regularizer as the combination of DBA and WHP seems to enable one of the hypotheses to find its way out of a local minimum, underscoring the synergistic impact of Penalized Diversity.

**WHP mitigates the negative influence of weak hypotheses** We studied the effect of anchor selection in the target hypothesis disparity regularization. Assuming source and target hypotheses have separate backbones, the performance of our model under fixed, random, ensemble (average), and WHP anchor selection strategies are presented in Table 6. It

can be observed from Table 6 in several experiments, such as S  $\rightarrow$  T, in the presence of weak performing hypothesis, while an ensemble anchor without WHP is subject to convergence towards weak hypotheses, random anchor selection might mitigate this issue partially. However, our results suggest that WHP, through the penalization of outlier hypotheses, provides the most efficient protection against the negative impact of weak hypotheses by assigning them lower weights in the ensemble anchor.

Results on Office-31 dataset with three hypotheses indicate similar findings (see Table 7). Given three hypotheses, in all of the fixed, random, and ensemble anchor selection strategies, the impact of a weak hypothesis is inevitable in the overall performance. The results also indicate the instability of random strategy. For instance, in A  $\rightarrow$  W, randomly choosing an anchor improved the performance in comparison with fixed selection, while in D  $\rightarrow$  A, the model seems to converge toward the weak hypothesis. Our results on both natural and medical domains state that using WHP helps to mitigate the effects of weak hypotheses.

**Penalized Diversity relies on the synergy of DBA and WHP** We ablate different components of the proposed Penalized Diversity (PD) for test-time adaptation performance on the LIDC dataset in Table 8. Table 8 shows that using a *Fixed* anchor selection, as done in HDMI, can lead to catastrophic failure cases due to error accumulation towards a weak hypothesis, which deems *Fixed* a poor choice for anchor selection. It is important to note that the increase

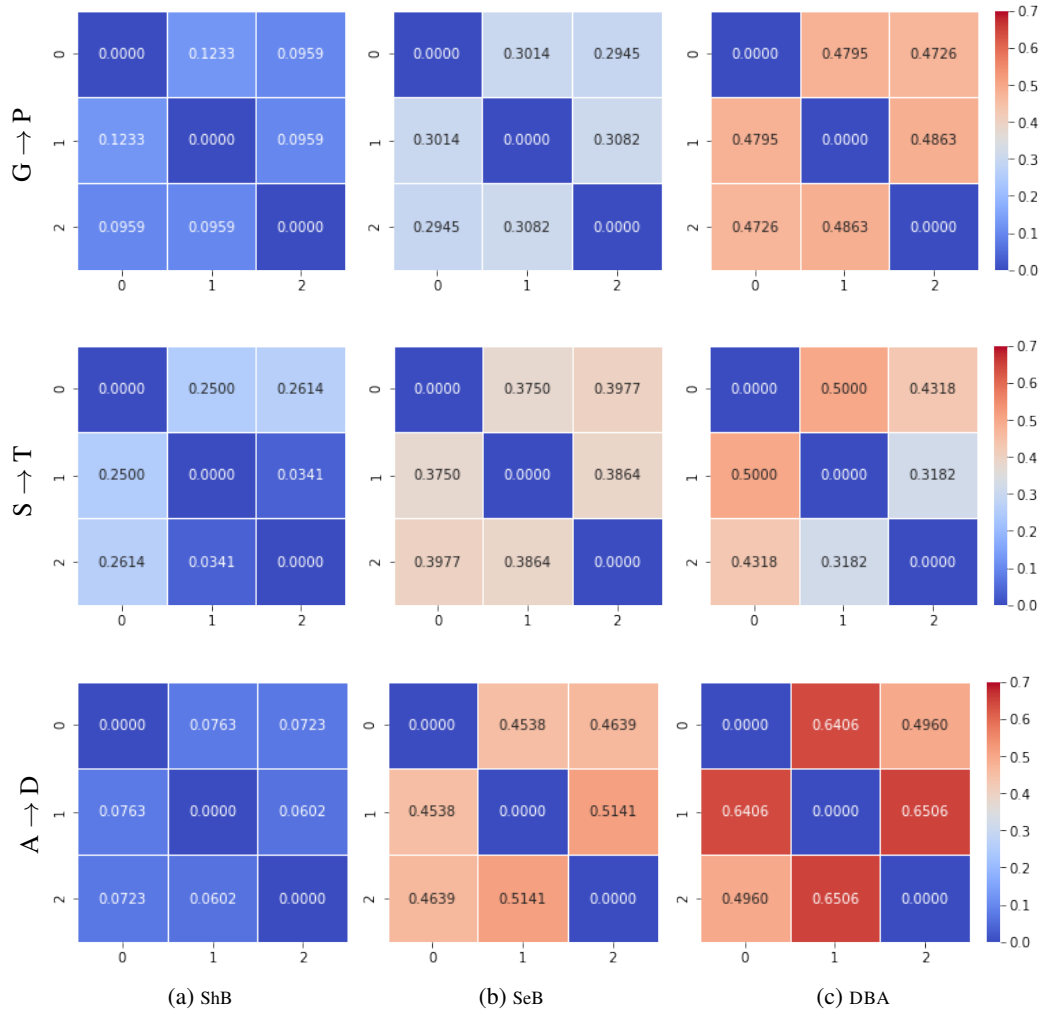


Figure 2: **Diversity of the source hypotheses** based on the choice of feature extraction backbone on  $G \rightarrow P$  (first row) and  $S \rightarrow T$  (second row) from LIDC, and  $A \rightarrow D$  from Office-31 datasets using disagreement of predictions between three hypotheses. *Left plot*: three hypotheses with shared features extractors (ShB). *Middle plot*: three hypotheses with separate feature extractors (no weight sharing) (SeB). *Right plot*: three hypotheses with distinct backbone (DBA).

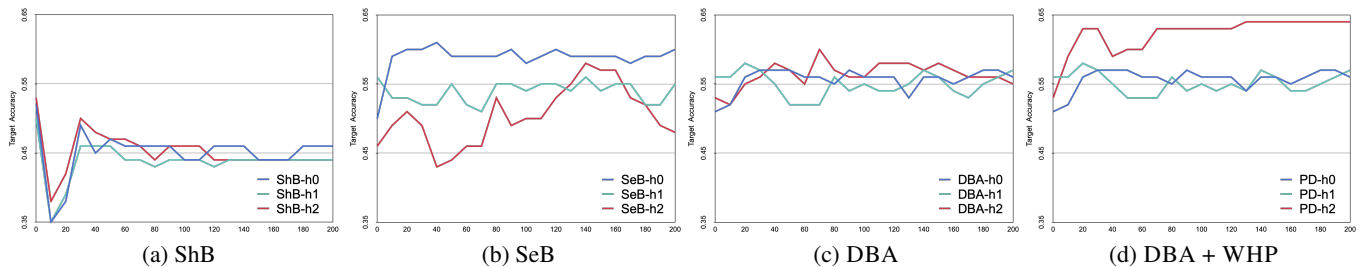


Figure 3: **Diversity of the target hypotheses during adaptation** based on the choice of feature extraction backbone on  $S \rightarrow T$  (LIDC). (a): three hypotheses that share feature extractor (ShB). (b): three hypotheses with separate feature extractors (SeB). (c): DBA with three independent hypotheses. (d): PD = DBA + WHP with three independent hypotheses (DBA).

in diversity seen in SeB and DBA (Fig. 2) results in worse performance when proper regularization is lacking (SeB +

Fixed and DBA + Fixed). It is only when WHP is introduced that we can mitigate the probability of convergence

Table 8: Ablation study on different components of PD = DBA + WHP under covariate shift. Target accuracy (%) on LIDC dataset using three hypotheses (source  $\rightarrow$  target). The results are averaged over five different runs.

Method	G $\rightarrow$ P	G $\rightarrow$ S	G $\rightarrow$ T	P $\rightarrow$ G	P $\rightarrow$ S	P $\rightarrow$ T	S $\rightarrow$ G	S $\rightarrow$ P	S $\rightarrow$ T	T $\rightarrow$ G	T $\rightarrow$ P	T $\rightarrow$ S	Avg.
ShB + Fixed	67.1	66.6	<b>64.6</b>	65.4	64.2	54.6	<b>66.2</b>	65.1	54.6	60.7	<b>60.0</b>	58.7	62.3
SeB + Fixed	66.7	64.4	57.3	64.5	63.3	53.2	65.2	66.4	55.5	60.4	59.9	57.8	61.2
DBA + Fixed	68.1	<b>66.5</b>	60.7	64.5	64.2	<b>55.5</b>	65.4	<b>67.8</b>	58.6	59.7	58.5	59.1	62.4
DBA +WHP	<b>68.9</b>	65.9	60.9	<b>65.6</b>	<b>65.6</b>	54.8	65.8	66.9	<b>66.6</b>	<b>61.2</b>	59.6	59.6	<b>63.5</b>

Table 9: Target accuracy (%) on digit datasets with minority-class ( $L_m$ ) label distribution shift with  $p = 0.1$  (source  $\rightarrow$  target). In these experiments, PD-NWMI refers to PD without the weighted MI maximization, and PD-T refers to PD with the true target class proportions as compared to class proportion generated via pseudo-labels.

Method	M $\rightarrow$ U	M $\rightarrow$ N	U $\rightarrow$ M	U $\rightarrow$ N	N $\rightarrow$ M	N $\rightarrow$ U	Avg.
PD-NWMI	65.9	46.5	61.3	25.3	68.5	62.7	55.0
PD	87.5	47.7	84.3	31.8	85.0	78.6	69.2
PD-T	92.4	52.4	85.1	31.8	87.1	80.7	71.6

towards weak hypotheses.

**Weighted MI mitigates label distribution shift** From Table 5, we observe that the performance of SHOT and HDMI dropped by more than 20% in  $L_m$  experiment in comparison with the covariate shift only experiment ( $N_i$ ) indicating the incapability of these models to perform under label distribution shift. Similarly, OSTAR and MARS which both designed to tackle label shift and unlike PD have access to the source data during adaptation, had more than 14% drop in their performance in  $L_m$  experiment. While our target estimation obtained from pseudo-labels is prone to errors, it significantly mitigates the catastrophic impact of label distribution shift by only 8% performance drop. The effect of our modified MI maximization is remarkable in  $L_t$  experiment where there is only 0.2% drop in the performance of PD in comparison with no label shift ( $N_i$ ). It should be noted that our earlier experiments showed that applying  $W$  to both label entropy,  $H(\hat{Y}^T)$ , and conditional entropy,  $H(\hat{Y}^T | X^T)$ , of MI maximization is no better than applying it solely to the label entropy.

**Estimated class proportions via pseudo-labels closely represent true class proportions in UDA** To evaluate the effect of weighted MI maximization in the performance of PD under label distribution shift, we compare the performance of PD with and without weighted MI maximization (PD-NWMI) on *Minority-Class shift* experiment. In this experiment, we choose 5 classes out of 10 in the target domain and changed their proportions by  $p = 0.1$ . Table 9 demonstrates a significant improvement (14%) on using estimated target class proportions under label distribution shift.

We further experiment on *Minority-Class shift* with the actual target class proportions. It can be observed from Table 9 that the performance of PD using the estimated target class proportions (PD) is close to true target class propor-

tions (PD-T) implying the effectiveness of pseudo-labeling.

### 3.6 Calibration Analysis

It has been shown that diverse ensemble models lead to the best-calibrated uncertainty estimators (Lakshminarayanan, Pritzel, and Blundell 2017). To evaluate the effect of diversity in PD from the calibration perspective, we compute the uncertainty and calibration of PD with Brier score (Brier et al. 1950) and Expected Calibration Error (ECE) (Naeini, Cooper, and Hauskrecht 2015) and compare it with two other unsupervised SFDA models.

For this experiment, we consider natural and synthetic datasets under covariate and label distribution shifts. It can be observed from Table 10, that PD performs well in terms of calibration metrics under covariate shift in natural dataset. We also compare the performance of SFDA models on digit datasets with covariate shift only and with both covariate and label distribution shifts. For the experiment with both covariate and label shifts, we compute the calibration metrics in *Minority-Class Shift* with  $p = 0.1$ . As seen from Table 10, changing the proportion of classes in the target domain not only negatively impacts the transferability of the other two unsupervised SFDA models but also worsens these models’ calibration. However, PD with a weighted MI maximization performs significantly better in terms of both performance and calibration after the introduction of label shift.

### 3.7 Sensitivity Analysis

**WHP is robust to hyper-parameter selection** To investigate the sensitivity of our model to the hyperparameter  $\beta$ , we conduct a set of experiments on A $\rightarrow$ D (Office-31) and G $\rightarrow$ P (LIDC) with three hypotheses and summarize the results in Fig. 4. For this experiment, we fix  $\alpha = 0.3$  for LIDC and  $\alpha = 1$  for Office-31. Setting  $\beta = 0$  reduces to solely maximizing mutual information. Fig 4 (a) and (b) show that introducing target training with WHP improved the performance in comparison with mutual information maximization ( $\beta = 0$ ). It is seen from the figure that despite the difference between the two domains (natural and medical), increasing the WHP contribution in target training improves the performance.

### 3.8 Ablation Study

**Choice of Different Architectures on PD** We study the effects of different architectural designs on the performance of PD as well as the diversity of the hypotheses. We compare two different choices of architectures for DBA. In this study,

Table 10: Calibration estimations for source-free domain adaptation models on the target domains  $A \rightarrow D$ , Office-31, and  $M \rightarrow U$  from digit dataset. Here  $N_l$  and  $L_m$  represent covariate shift only and covariate shift plus label distribution shift respectively. For the label distribution shift, we consider *Minority-Class shift* with  $p = 0.1$ . \* indicates calibration results reported from the original paper.

Model	Dataset	Shift	Target acc.	Brier Score ↓	ECE ↓
SHOT (Liang, Hu, and Feng 2020)			93.1	0.1246	0.0039
HDMI (Lao, Jiang, and Havaei 2021)*	$A \rightarrow D$	$N_l$	94.4	0.0961	0.0031
PD			95.6	<b>0.0771</b>	<b>0.0024</b>
SHOT (Liang, Hu, and Feng 2020)			88.9	0.2170	0.0072
HDMI (Lao, Jiang, and Havaei 2021)	$M \rightarrow U$	$N_l$	95.2	0.0926	0.0030
PD			96.9	<b>0.0567</b>	<b>0.0011</b>
SHOT (Liang, Hu, and Feng 2020)			57.1	0.8432	0.0279
HDMI (Lao, Jiang, and Havaei 2021)	$M \rightarrow U$	$L_m$	62.4	0.7417	0.0246
PD			87.5	<b>0.2467</b>	<b>0.0082</b>

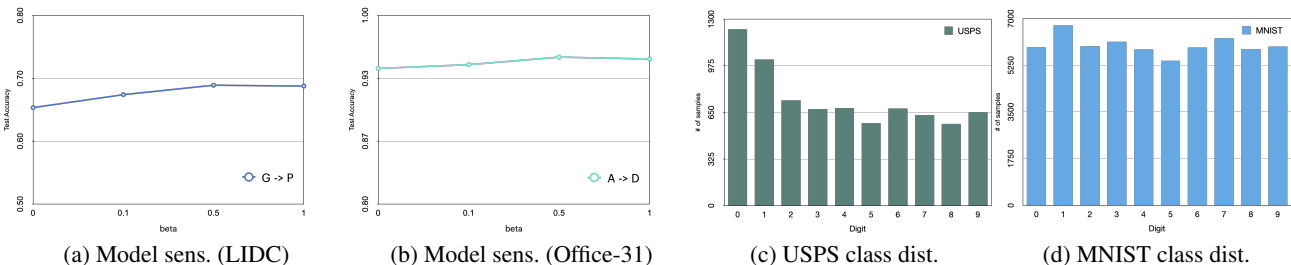


Figure 4: The two left plots show  $\beta$  sensitivity in  $G \rightarrow P$  (LIDC) and  $A \rightarrow D$  (Office-31) with three hypotheses. The two right plots indicate class distribution in USPS and MNIST datasets. Note that the class distribution of MNIST-M is the same as MNIST.

we simply consider different depths of a network as different backbones of PD (refers as A1). However, to investigate the performance of PD under totally different architectures, we consider a combination of SqueezeNet (Iandola et al. 2016) and ResNet in PD (refers as A2) with three hypotheses on LIDC. From Figure 5, we can observe that three hypotheses with entirely different architectures also improve the diversity. However, DBA without a proper regularizer creates uncontrolled diversity as shown in Figure 5(c). The experimental results presented in Table 11 show that imposing diversity on the model through entirely different architectural designs (i.e. A2) also leads to improvement in comparison with ShB with similar backbone architectures (from 62.3% to 62.8%).

## 4 Related Work

Transfer learning approaches can be divided into data-driven and model-driven approaches. Data-driven approaches such as instance weighting (Zadrozny 2004; Bickel, Brückner, and Scheffer 2007) and domain adaptation models such as DAN (Long et al. 2015), DANN (Ganin and Lempitsky 2015) and MDD (Zhang et al. 2019) assume to have direct access to the source data during the knowledge transfer. To mitigate transfer learning models’ privacy and storage concerns, source-free domain adaptation (SFDA) approaches (also known as model-driven or hypothesis transfer learning)

are proposed. SFDA is a transfer learning strategy where a model trained on the source domain incorporates the learning procedure of the target domain. It was first introduced by (Kuzborskij and Orabona 2013) where the access to the source domain was only limited to a set of hypotheses induced from it, unlike domain adaptation, where both source and target domains are used to adapt the source hypothesis to the target domain.

**Source-free Domain Adaptation** has been investigated from both practical and theoretical points of view in computer vision applications. Several studies have analyzed the effectiveness of SFDA on various specific ML algorithms (Kuzborskij and Orabona 2013, 2017; Wang and Schneider 2015), while others proposed more generally applicable frameworks (Fernandes and Cardoso 2019; Du et al. 2017). These studies can be divided based on the availability of labeled data in the target domain. Most previous studies considered the supervised SFDA setting (labeled target domain) (Kuzborskij and Orabona 2013, 2017; Wang and Schneider 2015; Fernandes and Cardoso 2019; Du et al. 2017), while unsupervised SFDA (uSFDA) (unlabeled target domain) has only recently gained interest (Liang, Hu, and Feng 2020; Lao, Jiang, and Havaei 2021). SFDA models mostly rely on a single hypothesis to transfer knowledge to the target domain. Lao, Jiang, and Havaei (2021) showed that using a single hypothesis for uSFDA is prone

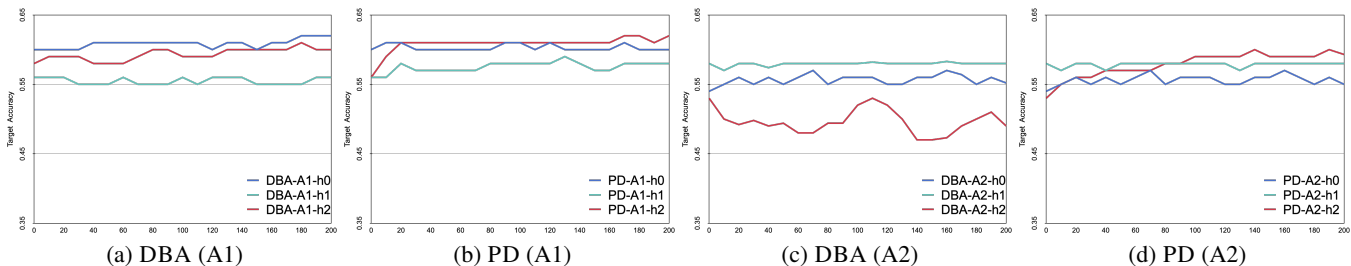


Figure 5: **Diversity of the target hypotheses during adaptation using various architecture choices** on  $T \rightarrow G$  from LIDC dataset. A1 represents the first choice of different backbone architectures including different depths of ResNet  $\{10, 18, 10\}$ . A2 represents the second choice of different backbone architectures including ResNet10, ResNet18, and SqueezeNet1.0. (a): DBA with three hypotheses and fixed anchor on the first architecture (A1). (b): PD with three hypotheses on the first architecture (A1). (c): DBA with three hypotheses and fixed anchor on the second architecture (A2). (d): PD with three hypotheses on the second architecture (A2).

Table 11: Ablation study on different architectural choices. Target accuracy (%) on LIDC dataset (source  $\rightarrow$  target) under covariate shift with two different choices of architectures; A1 and A2. The results are averaged over five different runs.

Method	G $\rightarrow$ P	G $\rightarrow$ S	G $\rightarrow$ T	P $\rightarrow$ G	P $\rightarrow$ S	P $\rightarrow$ T	S $\rightarrow$ G	S $\rightarrow$ P	S $\rightarrow$ T	T $\rightarrow$ G	T $\rightarrow$ P	T $\rightarrow$ S	Avg.
PD (A1)	<b>68.9</b>	<b>65.9</b>	60.9	<b>65.6</b>	<b>65.6</b>	54.8	<b>65.8</b>	<b>66.9</b>	<b>66.6</b>	<b>61.2</b>	<b>59.6</b>	<b>59.6</b>	<b>63.5</b>
PD (A2)	66.2	65.3	<b>64.3</b>	63.6	65.2	<b>59.1</b>	64.7	<b>66.9</b>	61.1	60.6	58.4	58.2	62.8

to overfitting the target domain and causes catastrophic forgetting of the source domain. They were the first to propose using multiple hypotheses to mitigate this effect. More recently Wang et al. (2022) proposed a novel way to tackle the SFDA problem by finding domain-invariant parameters rather than domain-invariant features in the model.

**Ensemble Models** Recently, deep neural network calibration gained considerable attention in the machine learning research community. Previous studies explored the effect of Monte Carlo dropout (Kingma, Salimans, and Welling 2015; Gal and Ghahramani 2016) and variational inference methods (Maddox et al. 2019). However, it has been shown that the best-calibrated uncertainty estimators can be achieved by neural network ensembles (Lakshminarayanan, Pritzel, and Blundell 2017; Ovadia et al. 2019; Ashukha et al. 2020). The importance of well-calibrated models becomes more important under the presence of dataset shift. The success of ensemble models is mainly related to the diversities present between their members. Ensemble diversity has been widely investigated in the literature (Brown 2004; Liu and Yao 1999). Improving diversity in neural network ensembles has become a focus in recent work. Stickland and Murray (2020) suggest augmenting each member of an ensemble with a different set of augmented input to increase the diversity among members. While a few recent studies propose deep ensemble models based on different neural network architectures to ensure diversity (Antorán, Allingham, and Hernández-Lobato 2020; Zaidi et al. 2020).

Recently Pagliardini et al. (2022) suggest that encouraging diversity between the ensemble predictions helps to generalize in the OOD setting by increasing disagreements and uncertainties over out-of-distribution samples. Whereas Lee, Yao, and Finn (2022) introduced an ensemble of multiple

hypotheses with shared feature extractors and separate classifier heads to generalize in the presence of spurious features. They proposed to increase diversity among the classifiers through mutual information minimization over the hypotheses predictions on unlabeled target data. Our work is different from (Pagliardini et al. 2022; Lee, Yao, and Finn 2022) in a sense that (i) to increase diversity, PD does not need a carefully selected set of target samples unlike both (Pagliardini et al. 2022; Lee, Yao, and Finn 2022), (ii) different from (Pagliardini et al. 2022) that limits the model to have a smaller or equal number of hypotheses than the total number of classes, we have freedom over the number of hypotheses in our model, and (iii) WHP mitigate weak hypotheses to improve overall performance without requiring access to labeled target samples as opposed to the active query strategy presented in (Lee, Yao, and Finn 2022). Despite its performance, PD also has its own limitation. Its diversification and penalization approaches force PD to be more effective with an ensemble of at least three hypotheses.

**Label Distribution Shift** Many domain adaptation studies focus only on covariate shift. Despite the negative impact of label distribution shift in transferring knowledge, it has been mostly neglected. Learning domain-invariant representations and using estimated class ratios between domains as importance weights in the training loss became a dominant strategy for many recent practices (Gong et al. 2016; Tachet des Combes et al. 2020; Shui et al. 2021). Rakotomamonjy et al. (2022) proposed MARS to learn domain-invariant representations with sample re-weighting. Several studies attempt to benefit optimal transport (OT) to find a transport function from source to target with a minimum cost. Kirchmeyer et al. (2022) proposed a reweighting model which maps pretrained representations using OT. The key

difference between these models and our modified MI solution is that they all assume accessing the source data during adaptation and their reweighing strategies are mainly based on source and target ratios.

## 5 Conclusion

This paper shows the benefits of increasing diversity in unsupervised source-free domain adaptation. We increased diversity by introducing separate feature extractors with Distinct Backbone Architectures (DBA) across hypotheses. With the support of experiments on various domains, we show that diversification must be accompanied by proper Weak Hypothesis mitigation through Penalization (WHP). Our proposed Penalized Diversity (PD) stems from the synergy of DBA and WHP. We further modified MI maximization in the objective of PD to account for the label shift problem. Our experiments on natural, synthetic, and medical benchmarks demonstrate how it improves upon the relevant baselines under different distributional shifts. As for future work, we would like to investigate other ways to promote diversity in the feature space of SFDA models.

## References

- Antorán, J.; Allingham, J.; and Hernández-Lobato, J. M. 2020. Depth uncertainty in neural networks. *Advances in neural information processing systems*, 33: 10620–10634.
- Armato III, S. G.; McLennan, G.; Bidaut, L.; McNitt-Gray, M. F.; Meyer, C. R.; Reeves, A. P.; Zhao, B.; Aberle, D. R.; Henschke, C. I.; Hoffman, E. A.; et al. 2011. The lung image database consortium (LIDC) and image database resource initiative (IDRI): a completed reference database of lung nodules on CT scans. *Medical physics*, 38(2): 915–931.
- Ashukha, A.; Lyzhov, A.; Molchanov, D.; and Vetrov, D. 2020. Pitfalls of In-Domain Uncertainty Estimation and Ensembling in Deep Learning. In *International Conference on Learning Representations*.
- Azizzadenesheli, K.; Liu, A.; Yang, F.; and Anandkumar, A. 2019. Regularized Learning for Domain Adaptation under Label Shifts. In *International Conference on Learning Representations*.
- Bahdanau, D.; Chorowski, J.; Serdyuk, D.; Brakel, P.; and Bengio, Y. 2016. End-to-end attention-based large vocabulary speech recognition. In *2016 IEEE international conference on acoustics, speech and signal processing (ICASSP)*, 4945–4949. IEEE.
- Bickel, S.; Brückner, M.; and Scheffer, T. 2007. Discriminative learning for differing training and test distributions. In *Proceedings of the 24th international conference on Machine learning*, 81–88.
- Brier, G. W.; et al. 1950. Verification of forecasts expressed in terms of probability. *Monthly weather review*, 78(1): 1–3.
- Brown, G. 2004. *Diversity in Neural Network Ensembles*. Ph.D. thesis, University of Birmingham, United Kingdom. Winner, British Computer Society Distinguished Dissertation Award.
- Dawid, A. P. 1982. The well-calibrated Bayesian. *Journal of the American Statistical Association*, 77(379): 605–610.
- Deng, Z.; Luo, Y.; and Zhu, J. 2019. Cluster alignment with a teacher for unsupervised domain adaptation. In *Proceedings of the IEEE/CVF International Conference on Computer Vision*, 9944–9953.
- Du, S. S.; Koushik, J.; Singh, A.; and Póczos, B. 2017. Hypothesis transfer learning via transformation functions. *Advances in neural information processing systems*, 30.
- Fernandes, K.; and Cardoso, J. S. 2019. Hypothesis transfer learning based on structural model similarity. *Neural Computing and Applications*, 31(8): 3417–3430.
- Fort, S.; Hu, H.; and Lakshminarayanan, B. 2019. Deep ensembles: A loss landscape perspective. *arXiv preprint arXiv:1912.02757*.
- Gal, Y.; and Ghahramani, Z. 2016. Dropout as a Bayesian approximation: Representing model uncertainty in deep learning. In *international conference on machine learning*, 1050–1059. PMLR.
- Ganin, Y.; and Lempitsky, V. 2015. Unsupervised domain adaptation by backpropagation. In *International conference on machine learning*, 1180–1189. PMLR.
- Ganin, Y.; Ustinova, E.; Ajakan, H.; Germain, P.; Larochelle, H.; Laviolette, F.; Marchand, M.; and Lempitsky, V. 2016. Domain-adversarial training of neural networks. *The journal of machine learning research*, 17(1): 2096–2030.
- Geirhos, R.; Jacobsen, J.-H.; Michaelis, C.; Zemel, R.; Brendel, W.; Bethge, M.; and Wichmann, F. A. 2020. Shortcut learning in deep neural networks. *Nature Machine Intelligence*, 2(11): 665–673.
- Gong, M.; Zhang, K.; Liu, T.; Tao, D.; Glymour, C.; and Schölkopf, B. 2016. Domain adaptation with conditional transferable components. In *International conference on machine learning*, 2839–2848. PMLR.
- Guan, H.; and Liu, M. 2021. Domain adaptation for medical image analysis: a survey. *IEEE Transactions on Biomedical Engineering*.
- He, K.; Zhang, X.; Ren, S.; and Sun, J. 2016. Deep residual learning for image recognition. In *Proceedings of the IEEE conference on computer vision and pattern recognition*, 770–778.
- Hull, J. J. 1994. A database for handwritten text recognition research. *IEEE Transactions on pattern analysis and machine intelligence*, 16(5): 550–554.
- Iandola, F. N.; Han, S.; Moskewicz, M. W.; Ashraf, K.; Dally, W. J.; and Keutzer, K. 2016. SqueezeNet: AlexNet-level accuracy with 50x fewer parameters and 0.5 MB model size. *arXiv preprint arXiv:1602.07360*.
- Jin, Y.; Wang, X.; Long, M.; and Wang, J. 2020. Minimum class confusion for versatile domain adaptation. In *European Conference on Computer Vision*, 464–480. Springer.
- Karani, N.; Chaitanya, K.; Baumgartner, C.; and Konukoglu, E. 2018. A lifelong learning approach to brain MR segmentation across scanners and protocols. In *International Conference on Medical Image Computing and Computer-Assisted Intervention*, 476–484. Springer.

- Kingma, D. P.; Salimans, T.; and Welling, M. 2015. Variational dropout and the local reparameterization trick. *Advances in neural information processing systems*, 28.
- Kirchmeyer, M.; Rakotomamonjy, A.; de Bezenac, E.; and patrick gallinari. 2022. Mapping conditional distributions for domain adaptation under generalized target shift. In *International Conference on Learning Representations*.
- Kornblith, S.; Norouzi, M.; Lee, H.; and Hinton, G. 2019. Similarity of neural network representations revisited. In *International Conference on Machine Learning*, 3519–3529. PMLR.
- Kuzborskij, I.; and Orabona, F. 2013. Stability and hypothesis transfer learning. In *International Conference on Machine Learning*, 942–950. PMLR.
- Kuzborskij, I.; and Orabona, F. 2017. Fast rates by transferring from auxiliary hypotheses. *Machine Learning*, 106(2): 171–195.
- Lakshminarayanan, B.; Pritzel, A.; and Blundell, C. 2017. Simple and scalable predictive uncertainty estimation using deep ensembles. *Advances in neural information processing systems*, 30.
- Lao, Q.; Jiang, X.; and Havaei, M. 2021. Hypothesis disparity regularized mutual information maximization. In *Proceedings of the AAAI Conference on Artificial Intelligence*, volume 35, 8243–8251.
- LeCun, Y.; Bottou, L.; Bengio, Y.; and Haffner, P. 1998. Gradient-based learning applied to document recognition. *Proceedings of the IEEE*, 86(11): 2278–2324.
- Lee, Y.; Yao, H.; and Finn, C. 2022. Diversify and Disambiguate: Learning From Underspecified Data. *arXiv preprint arXiv:2202.03418*.
- Li, Y.; Wang, N.; Shi, J.; Liu, J.; and Hou, X. 2016. Revisiting batch normalization for practical domain adaptation. *arXiv preprint arXiv:1603.04779*.
- Liang, J.; Hu, D.; and Feng, J. 2020. Do we really need to access the source data? source hypothesis transfer for unsupervised domain adaptation. In *International Conference on Machine Learning*, 6028–6039. PMLR.
- Liu, Y.; and Yao, X. 1999. Ensemble learning via negative correlation. *Neural networks*, 12(10): 1399–1404.
- Long, M.; Cao, Y.; Wang, J.; and Jordan, M. 2015. Learning transferable features with deep adaptation networks. In *International conference on machine learning*, 97–105. PMLR.
- Long, M.; Cao, Z.; Wang, J.; and Jordan, M. I. 2018. Conditional adversarial domain adaptation. *Advances in neural information processing systems*, 31.
- Maddox, W. J.; Izmailov, P.; Garipov, T.; Vetrov, D. P.; and Wilson, A. G. 2019. A simple baseline for Bayesian uncertainty in deep learning. *Advances in Neural Information Processing Systems*, 32.
- Naeini, M. P.; Cooper, G.; and Hauskrecht, M. 2015. Obtaining well calibrated probabilities using Bayesian binning. In *Twenty-Ninth AAAI Conference on Artificial Intelligence*.
- Nguyen, T.; Raghu, M.; and Kornblith, S. 2021. Do Wide and Deep Networks Learn the Same Things? Uncovering How Neural Network Representations Vary with Width and Depth. In *International Conference on Learning Representations*.
- Ovadia, Y.; Fertig, E.; Ren, J.; Nado, Z.; Sculley, D.; Nowozin, S.; Dillon, J.; Lakshminarayanan, B.; and Snoek, J. 2019. Can you trust your model’s uncertainty? evaluating predictive uncertainty under dataset shift. *Advances in neural information processing systems*, 32.
- Pagliardini, M.; Jaggi, M.; Fleuret, F.; and Karimireddy, S. P. 2022. Agree to Disagree: Diversity through Disagreement for Better Transferability. *arXiv preprint arXiv:2202.04414*.
- Peng, X.; Usman, B.; Kaushik, N.; Wang, D.; Hoffman, J.; and Saenko, K. 2018. Visda: A synthetic-to-real benchmark for visual domain adaptation. In *Proceedings of the IEEE Conference on Computer Vision and Pattern Recognition Workshops*, 2021–2026.
- Quiñonero-Candela, J.; Sugiyama, M.; Schwaighofer, A.; and Lawrence, N. D. 2008. *Dataset shift in machine learning*. Mit Press.
- Rakotomamonjy, A.; Flamary, R.; Gasso, G.; Alaya, M. E.; Berar, M.; and Courty, N. 2022. Optimal transport for conditional domain matching and label shift. *Machine Learning*, 111(5): 1651–1670.
- Rame, A.; and Cord, M. 2021. DICE: Diversity in Deep Ensembles via Conditional Redundancy Adversarial Estimation. In *International Conference on Learning Representations*.
- Russakovsky, O.; Deng, J.; Su, H.; Krause, J.; Satheesh, S.; Ma, S.; Huang, Z.; Karpathy, A.; Khosla, A.; Bernstein, M.; et al. 2015. Imagenet large scale visual recognition challenge. *International journal of computer vision*, 115(3): 211–252.
- Saenko, K.; Kulis, B.; Fritz, M.; and Darrell, T. 2010. Adapting visual category models to new domains. In *European conference on computer vision*, 213–226. Springer.
- Shui, C.; Li, Z.; Li, J.; Gagné, C.; Ling, C. X.; and Wang, B. 2021. Aggregating from multiple target-shifted sources. In *International Conference on Machine Learning*, 9638–9648. PMLR.
- Stacke, K.; Eilertsen, G.; Unger, J.; and Lundström, C. 2019. A closer look at domain shift for deep learning in histopathology. *arXiv preprint arXiv:1909.11575*.
- Stickland, A. C.; and Murray, I. 2020. Diverse ensembles improve calibration. *arXiv preprint arXiv:2007.04206*.
- Tachet des Combes, R.; Zhao, H.; Wang, Y.-X.; and Gordon, G. J. 2020. Domain adaptation with conditional distribution matching and generalized label shift. *Advances in Neural Information Processing Systems*, 33: 19276–19289.
- Turner, K.; and Oza, N. C. 1999. Decimated input ensembles for improved generalization. In *IJCNN’99. International Joint Conference on Neural Networks. Proceedings (Cat. No. 99CH36339)*, volume 5, 3069–3074. IEEE.

- Vaswani, A.; Shazeer, N.; Parmar, N.; Uszkoreit, J.; Jones, L.; Gomez, A. N.; Kaiser, Ł.; and Polosukhin, I. 2017. Attention is all you need. *Advances in neural information processing systems*, 30.
- Venkateswara, H.; Eusebio, J.; Chakraborty, S.; and Panchanathan, S. 2017. Deep hashing network for unsupervised domain adaptation. In *Proceedings of the IEEE conference on computer vision and pattern recognition*, 5018–5027.
- Wang, D.; Shelhamer, E.; Liu, S.; Olshausen, B.; and Darrell, T. 2021. Tent: Fully Test-Time Adaptation by Entropy Minimization. In *International Conference on Learning Representations*.
- Wang, F.; Han, Z.; Gong, Y.; and Yin, Y. 2022. Exploring Domain-Invariant Parameters for Source Free Domain Adaptation. In *Proceedings of the IEEE/CVF Conference on Computer Vision and Pattern Recognition*, 7151–7160.
- Wang, X.; and Schneider, J. G. 2015. Generalization Bounds for Transfer Learning under Model Shift. In *UAI*, 922–931.
- Xu, R.; Li, G.; Yang, J.; and Lin, L. 2019. Larger norm more transferable: An adaptive feature norm approach for unsupervised domain adaptation. In *Proceedings of the IEEE/CVF International Conference on Computer Vision*, 1426–1435.
- Yang, S.; van de Weijer, J.; Herranz, L.; Jui, S.; et al. 2021. Exploiting the intrinsic neighborhood structure for source-free domain adaptation. *Advances in Neural Information Processing Systems*, 34: 29393–29405.
- Zadrozny, B. 2004. Learning and evaluating classifiers under sample selection bias. In *Proceedings of the twenty-first international conference on Machine learning*, 114.
- Zaidi, S.; Zela, A.; Elsken, T.; Holmes, C.; Hutter, F.; and Teh, Y. W. 2020. Neural ensemble search for performant and calibrated predictions. *arXiv preprint arXiv:2006.08573*, 2: 3.
- Zaidi, S.; Zela, A.; Elsken, T.; Holmes, C. C.; Hutter, F.; and Teh, Y. 2021. Neural ensemble search for uncertainty estimation and dataset shift. *Advances in Neural Information Processing Systems*, 34.
- Zhang, Y.; Liu, T.; Long, M.; and Jordan, M. 2019. Bridging theory and algorithm for domain adaptation. In *International Conference on Machine Learning*, 7404–7413. PMLR.

## A Appendix

### A.1 Experimental Setup

For the medical dataset, we used different depths of 3D-ResNet as the hypothesis backbone, mainly ResNet10 and ResNet18. Each backbone  $\{\phi_i\}_{i=1}^M$  is then followed by a set of fully connected layers, Batch-Norm, ReLU activation function, and Dropout referred to as the bottleneck layer. We used 512 as the dimension of extracted features. For the classifier  $\{f_i\}_{i=1}^M$ , we used a shallow neural network with two fully connected layers, followed by a ReLU activation function, and Dropout. Each model trained for 200 iterations with batch size 32 and learning rate  $1e-4$  and AdamW optimizer on the source domain. We used the same configuration for the target training except the learning rate was decreased to  $1e-5$ . For the experiments with 3 hypotheses, we used ResNet  $\{10, 18, 10\}$ , indicating the depth of each feature extractor. For the baselines, we used the same configuration with ResNet18 as their backbone whether they have single or multiple hypotheses.  $\alpha = 0.3$  and  $\beta = 0.5$  are used for the target training.

For natural images datasets, we use different depths of ResNet (He et al. 2016) pre-trained on ImageNet (Russakovsky et al. 2015) as the backbone of our feature extractors. Specifically, ResNet of depths  $\{34, 50, 34\}$  for Office-31 and Office-Home and ResNet of depths  $\{50, 101, 110\}$  for VisDA-C are chosen as the depths of  $\{g_i\}_{i=1}^M$  for  $M = 3$  hypotheses. The same bottleneck layer as our experiments on medical data is used for the experiments on natural images. We followed similar hyperparameters as (Liang, Hu, and Feng 2020) for synthetic digit datasets with different depths on PD. For both natural and synthetic datasets, we trained the source hypotheses for 5k iterations, with learning rate  $3e-4$  and batch size of 64. Target hypotheses are trained for 20k iterations with learning rate  $3e-4$  and batch size of 64. We used SGD optimizer for both source and target training. We used  $\alpha = 1$  and  $\beta = 0.5$  for the target training objective function.

For the experiments on digit datasets, we used  $p = 0.1$  as the probability value of changing the chosen class, i.e. a class with 1000 samples in the target domain will be reduced to 100 samples in the new shifted domain.

### A.2 Statistical Analysis on LIDC Covariate Shift

The Lung Image Database Consortium (LIDC) (Armato III et al. 2011) consists of diagnostic and lung cancer screening thoracic computed tomography (CT) scans. The images are captured in multiple institutions with imaging devices produced by four different manufacturers. It has been shown that images from different institutions as well as hardware differences in data acquisition devices are susceptible to domain shift (also known as covariate shift) (Guan and Liu 2021; Stacke et al. 2019; Karani et al. 2018). We suggested dividing the LIDC dataset into four sub-datasets based on the imaging device manufacturer. Each of these sub-datasets introduces one domain. Aside from the results presented in Table 3 of the paper (Sec. 3.4, results on LIDC under covariate shift) obtained by the Source-only model, this section

provides a statistical argument for the existence of a covariate shift in our suggested approach.

Assuming that each of the sub-datasets (i.e. domain) is different from the others introducing a comparative observational study or experiment, we assess the difference between proportions or means of each two experiments.

Given the performance of the Source-only model on each domain within five different runs, we computed the confidence interval (CI) between each two population proportions using Eq. 11.

$$CI = P \text{ difference} \pm SE \text{ for Difference} \quad (11)$$

and

$$\begin{aligned} P \text{ difference} &= pr_{d_1} - pr_{d_2} \\ SE \text{ for Difference} &= \sqrt{(SE_{p_1})^2 + (SE_{p_2})^2} \end{aligned} \quad (12)$$

where  $SE$  for proportion  $p_i$  defines standard error and it is computed as follows:

$$SE_{p_i} = \sqrt{\frac{pr_{d_i}(1 - pr_{d_i})}{N_{p_i}}}$$

where  $N_{p_i}$  indicates the total number of samples in each proportion/domain, and  $pr_{d_i}$  is the accuracy of Source-only model trained on the proportion  $p_i$ .

If two CIs do not overlap, then it can be said that there is a statistically significant difference between the two populations. In another word, if the confidence interval for the difference does not contain zero, we can confirm the existence of covariate shift between two domains.

The highlighted values in Table 12 indicate overlaps between two domains on a particular run. As seen from Table 12, the highest domain shift is observed between T and the other domains. These findings are also aligned with the results reported in the paper on the LIDC dataset, where the lowest performance is obtained where T is either source or target domain (see Table 3). Since in nearly all the experiments, at least four out of five experiments show no overlaps, we conclude that our suggested approach to creating sub-datasets indeed maintains domain shift.

Table 12: The confidence interval (CI) on each domain using the Source-only model on LIDC dataset with covariate shift.

Source	Run	G	P	S	T
G	S1	–	<b>(-0.09, 2.95)</b>	(-5.66, -0.20)	(17.63, 21.69)
	S2	–	(-4.96, -1.98)	<b>(-1.71, 3.85)</b>	(12.53, 16.59)
	S3	–	(0.67, 3.73)	(-5.53, -0.05)	(18.18, 22.24)
	S4	–	(0.36, 3.40)	(-6.15, -0.73)	(18.10, 22.15)
	S5	–	(3.85, 6.95)	(1.22, 6.90)	(19.10, 23.14)
P	S1	<b>(-2.10, 0.14)</b>	–	<b>(-3.32, 0.74)</b>	(6.10, 12.62)
	S2	(3.15, 6.15)	–	(6.50, 10.48)	(15.25, 21.73)
	S3	(0.76, 3.82)	–	(1.89, 5.89)	(11.13, 17.63)
	S4	(-3.53, -0.51)	–	<b>(-1.26, 2.70)</b>	(12.27, 18.77)
	S5	(3.33, 6.45)	–	(1.53, 5.57)	(10.21, 16.72)
S	S1	(-3.17, -3.13)	<b>(-0.00, 5.70)</b>	–	(2.39, 8.85)
	S2	(1.07, 4.11)	(-7.61, -2.27)	–	(5.57, 12.01)
	S3	(1.25, 4.27)	(-6.39, -1.05)	–	(9.05, 15.51)
	S4	(-6.10, -3.05)	(-10.85, -5.45)	–	(5.05, 11.55)
	S5	(-5.42, -2.36)	(-5.72, -0.12)	–	<b>(-5.33, 0.97)</b>
T	S1	(18.93, 21.97)	(17.57, 23.33)	(18.44, 22.46)	–
	S2	(18.93, 21.97)	(71.57, 23.33)	(18.44, 22.46)	–
	S3	(22.36, 25.36)	(21.0, 26.72)	(21.87, 25.85)	–
	S4	(17.79, 20.85)	(16.44, 22.20)	(17.31, 21.33)	–
	S5	(17.79, 20.85)	(16.44, 22.20)	(17.31, 21.33)	–